LOGO: A hybrid approach for calibration of crop model parameters using local and global methods in tandem

Supplementary information 1

Synthetic observational data were generated to represent diverse climate conditions (Fig. S1). The sites where observation data were obtained had different Köppen-Geiger climate classification (Fig. S2).

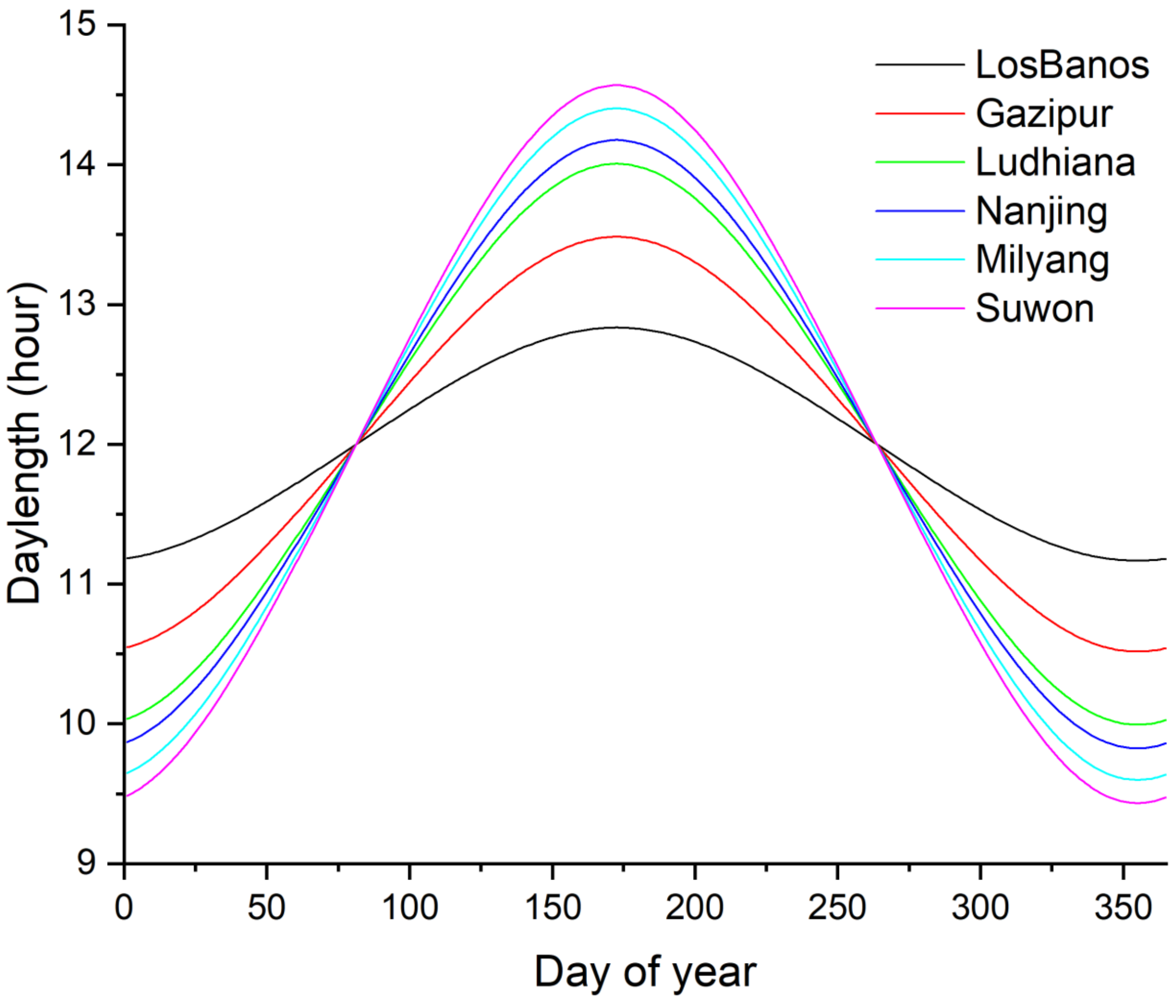

Fig. S1. Change of daylength at the sites of interest.

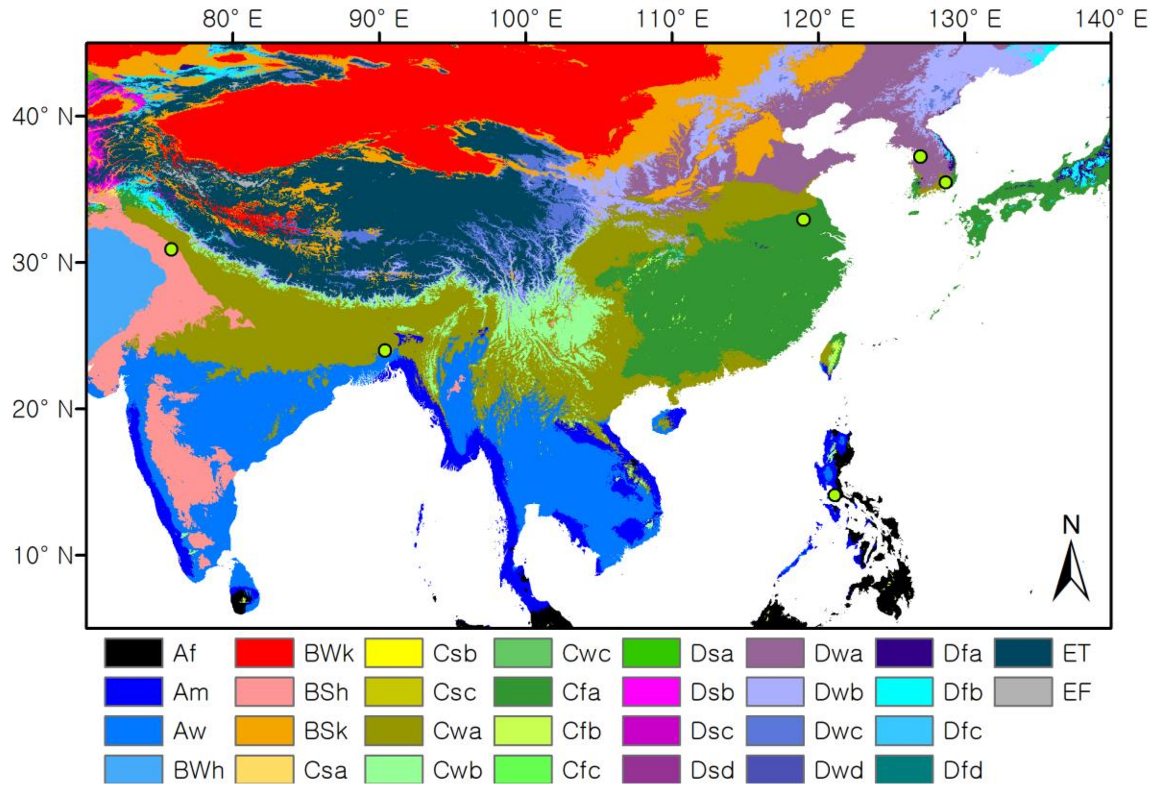

Fig. S2. Köppen climate classification for the experiment sites indicated by dot. The map of climate classification was suggested by Beck et al. (2023).

Supplementary information 2

The ranges of parameters values were determined using the default values included in the input files to the CERES-Rice model (Table S1).

Table S1. Lower and upper bound of the parameter used for calibration

Group	Type	Parameter	Lower bound	Upper bound
Phenology	Major	P2R	5	300
	Major	PHINT	55	90
	Major	P5	150	850
	Candidate	P1	150	800
	Candidate	P2O	11	13
	Candidate	TCLDP	12	18
Biomass	Major	G3	0.7	1.3
Grain number	Major	G1	50	80
Yield	Major	G2	0.015	0.03
	Candidate	THOT	25	34
	Candidate	TCLDF	10	20

Supplementary information 3

When the Manhattan distance between true and estimated parameter sets was less than 0.5, the maximum errors in heading date and yield were 2% and 5%, respectively (Fig. S3). The Mean Absolute Error (MAE) for heading date and the Normalized Root Mean Square Error (NRMSE) for yield tended to increase with increasing values of $D_{o,e}$.

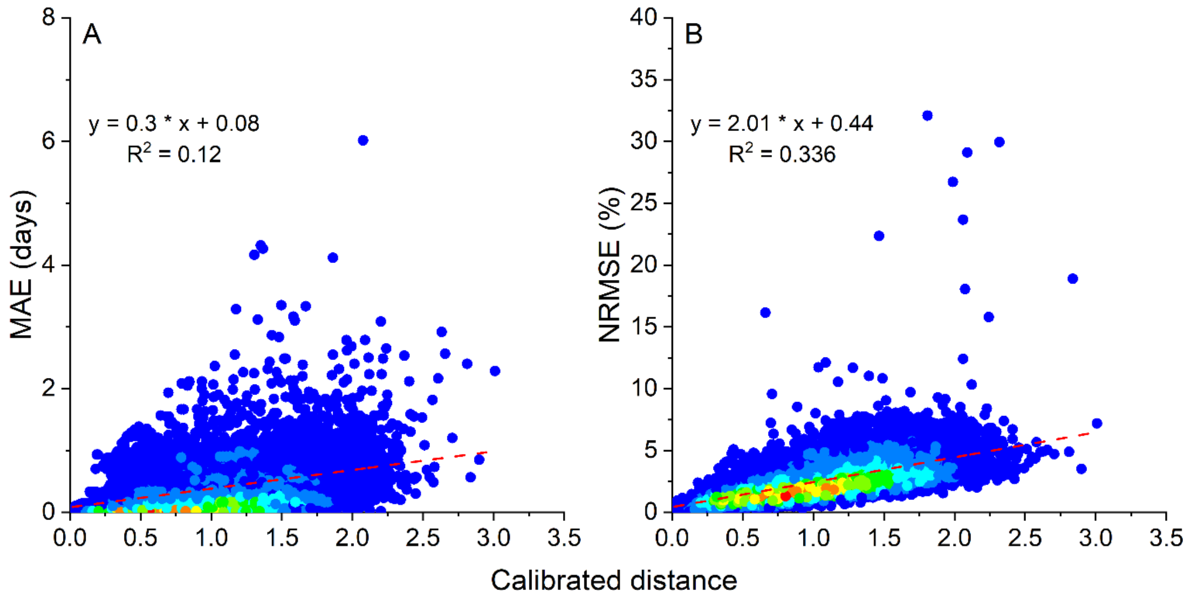

Fig. S3. Relationship between the distance of parameter estimates from the true parameter and the model error for (A) heading date and (B) yield at maturity, respectively.

Supplementary information 4

Table S2. Evaluation of the simulated phenology and growth variables using the parameter set obtained from LOGO algorithm

	2 sites	3 sites	4 sites	5 sites
Heading date				
R^2	0.996	0.996	0.998	0.996
MAE (days)	0.53	0.6	0.25	0.47
Maturity date				
R^2	0.996	0.995	0.998	0.996
MAE (days)	0.65	0.67	0.28	0.68
Biomass				
R^2	0.997	0.998	0.999	0.998
RMSE (kg ha^{-1})	128	109	106	87.4
Grain number				
R^2	0.99	0.993	0.996	0.997
RMSE (number m^{-2})	956.5	1847.8	1661.1	939.3
Yield				
R^2	0.99	0.993	0.996	0.997
RMSE (kg ha^{-1})	151.35	120.23	109.86	84.52

Supplementary information 5

It would be challenging to estimate parameter values close to the true values using calibration based solely on global search algorithms. For example, calibration using the GLUE method resulted in a distance around 0.97 (Fig. S4), when evaluating 10^6 random parameter sets. Moreover, the sensitivity of the calibration results to the order of sampled parameter sets was evaluated to account for the random sampling effects. The 10^6 parameter sets were divided into 10 groups of 10^5 parameter sets each, and calibration was performed using cumulative combinations of the groups. The distance between the calibrated and true parameter values tended to stabilize as the number of the sampled parameter groups increased. Still, in some cases, additional sampling resulted in the parameter estimates to be more distant from the true parameter set. This is due to the presence of multiple parameter sets that provide similarly good fits to the calibration data, making it difficult to identify parameter values close to the true parameter set using a global sampling framework alone.

It becomes more challenging as the number of parameters increases. Approaches based on global sampling explore the entire parameter space, the volume of which grows exponentially with dimensionality. Thus, substantially more parameter sets are required to obtain a reliable approximation of the parameter distribution (Makowski et al., 2002). In contrast, local optimization methods may help mitigate this issue. Although a parameter appears optimal when considered individually, such points are often saddle points in high-dimensional parameter space, allowing further progress in the optimization process (Dauphin et al., 2014). These results suggest that combining local and global methods would be advantageous for robust parameter estimation.

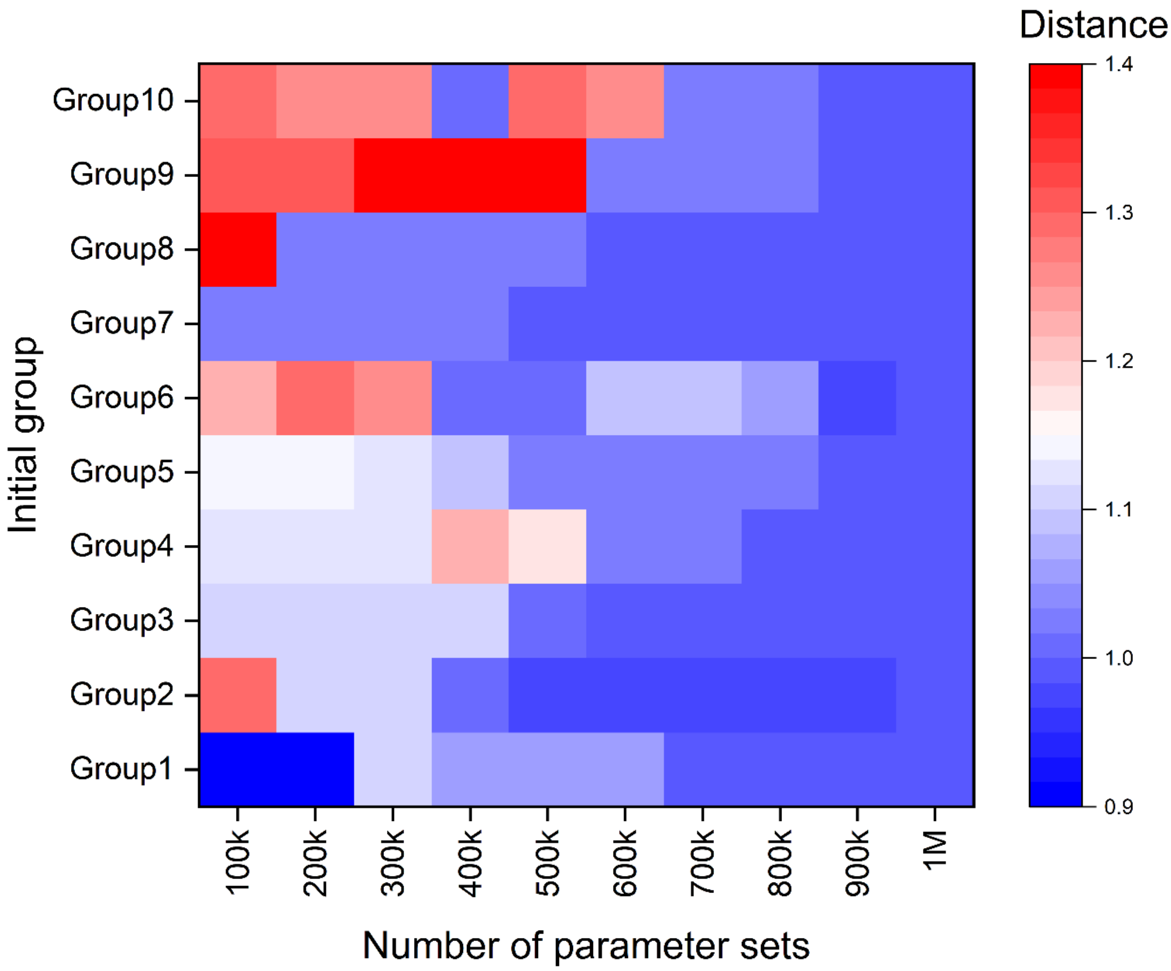

Fig. S4. Distance between the true and calibrated parameter sets with increasing sample size using the GLUE method. The random parameter sets were divided into 10 groups, and calibration results were evaluated by cumulatively increasing the number of groups starting from different groups.

Supplementary information 6

The LOGO algorithm was applied to the actual data to verify whether the proposed method produces reliable results under realistic conditions. The observation data were obtained from yield trials conducted in Korea for the wheat cultivar *Geumgang* (Table S3; Hyun et al., 2025). Phenology (heading and maturity) and yield were compiled from the experiments for crop yield reports at 45 site years. Weather data were obtained from the nearest weather stations operated by the Korea Meteorological Administration (https://data.kma.go.kr). Soil data were obtained from soil series data provided by Rural Development Administration (https://soil.rda.go.kr), with Sangju and Jisan selected as representative soils for upland and lowland fields, respectively.

Table S3. The list of site and years where wheat data were obtained in Korea

Site	Latitude (degree)	Years	Use
Yesan	36.777	2014, 2015, 2016, 2024	calibration
Daegu	35.878	2006, 2009, 2012, 2013, 2019	calibration
Jeonju	35.841	2005, 2006, 2007, 2009, 2010, 2011, 2013, 2014	calibration
Milyang	35.492	2010, 2015, 2018, 2019, 2022, 2023, 2024	calibration
Naju	35.173	2013, 2015, 2016, 2017, 2018, 2019, 2023	calibration
Jinju	35.164	2016, 2018, 2022, 2023	calibration
Suwon	37.258	2016, 2018, 2021, 2024	validation

Jeju	33.514	2011, 2018, 2021	validation

These data were used for parameter calibration of DSSAT-NWHEAT model using LOGO framework. The initial parameters were set within the range defined by Wallach et al. (2025) (Table S4). In total, eight sets of parameters for *YECORA ROJO*, *YECORA*, *Bacanora 88*, *Nesser*, *Spear*, *Wilgoyne*, *Gamenya*, and *Yitpi* cultivars were used for initial parameters. By the initial parameter, calibration was performed for combination of site subsets.

Table S4. Lower and upper bound of the parameter used for calibration

Group	Type	Parameter	Description (unit)	Lower bound	Upper bound
Phenology	Major	P1	Thermal time from emergence to the end of the juvenile phase (°C)	300	600
	Major	P5	Thermal time from beginning of grain fillling to maturity (°C)	200	800
	Candidate	VSEN	Sensitivity to vernalization (-)	1	5
	Candidate	PPSEN	Sensitivity to photoperiod (-)	1	5
	Candidate	PHINT	Phyllochron interval (°C)	70	120
Yield	Major	RUE1	Pre-anthesis radiation use efficiency (g MJ^{-1})	3	5
	Candidate	RUE2	Pre-anthesis radiation use efficiency (g MJ^{-1})	3	5
	Candidate	STMMX	Potential final dry weight of a	1	5

		single tiller excluding grain (g $stem^{-1}$)		
Candidate	P2AF	Threshold aeration deficit in a layer becoming effective on root growth (-)	0.4	0.8
Candidate	ADLAI	Threshold aeration deficit affecting LAI (-)	0.5	1
Candidate	PLGP1	Parameter for calculating potential leaf area growth (-)	1000	2000
Candidate	PLGP2	Parameter for calculating potential leaf area growth (-)	0.4	0.8
Candidate	SLAP1	Ratio of leaf area to mass at emergence (cm2 g^{-1})	250	400
Candidate	SLAP2	Ratio of leaf area to mass at end of leaf growth (cm2 g^{-1})	200	300
Candidate	MXNUP	Max N uptake per day (g m^{-2})	0.4	1
Candidate	GRNO	Coefficient of kernel number per stem weight at the beginning of grain filling (kernels g^{-1})	20	30
Candidate	STEMN	Fraction of C of stem to be translocated to grain (-)	0	1
Candidate	MXFIL	Potential kernel growth rate (mg / day)	1	3

	Candidate	INGNC	Initial grain N concentration (g N / g biomass)	0.01	0.04

It was found that the error caused by the parameter estimates was relatively small when the LOGO algorithm was applied (Fig. S5). The outcome of LOGO parameter estimation indicated that the NRMSE value was smaller for the combinations of four sites than that of the other number of sites. Although the RMSE value for such parameters was not necessarily smallest. Still, it was smaller than the median value of RMSE values derived using the parameter estimates under the given combination of five sites.

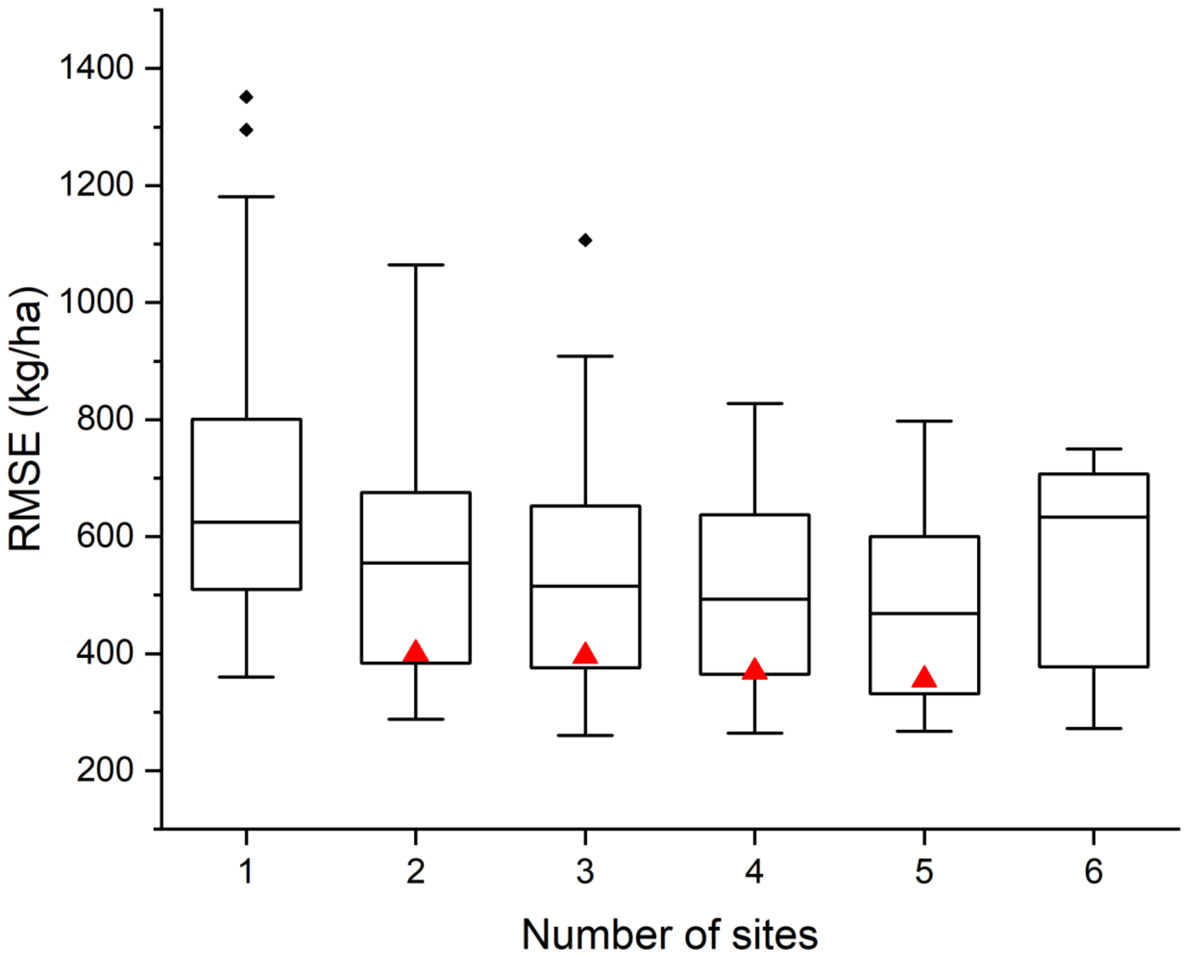

Fig. S5. Effect of the GLUE procedure on the error between the simulated and observed yields, compared to the calibration results using each site combination. The triangle represents the results from the LOGO algorithm.

In the validation sets, the estimated parameters resulted in smaller error than the default parameter sets (Fig. S6-S7). For example, the NRMSE value for crop yield was 3.5 % using the estimated parameters, whereas minimum 11.37 % using the default parameter sets.

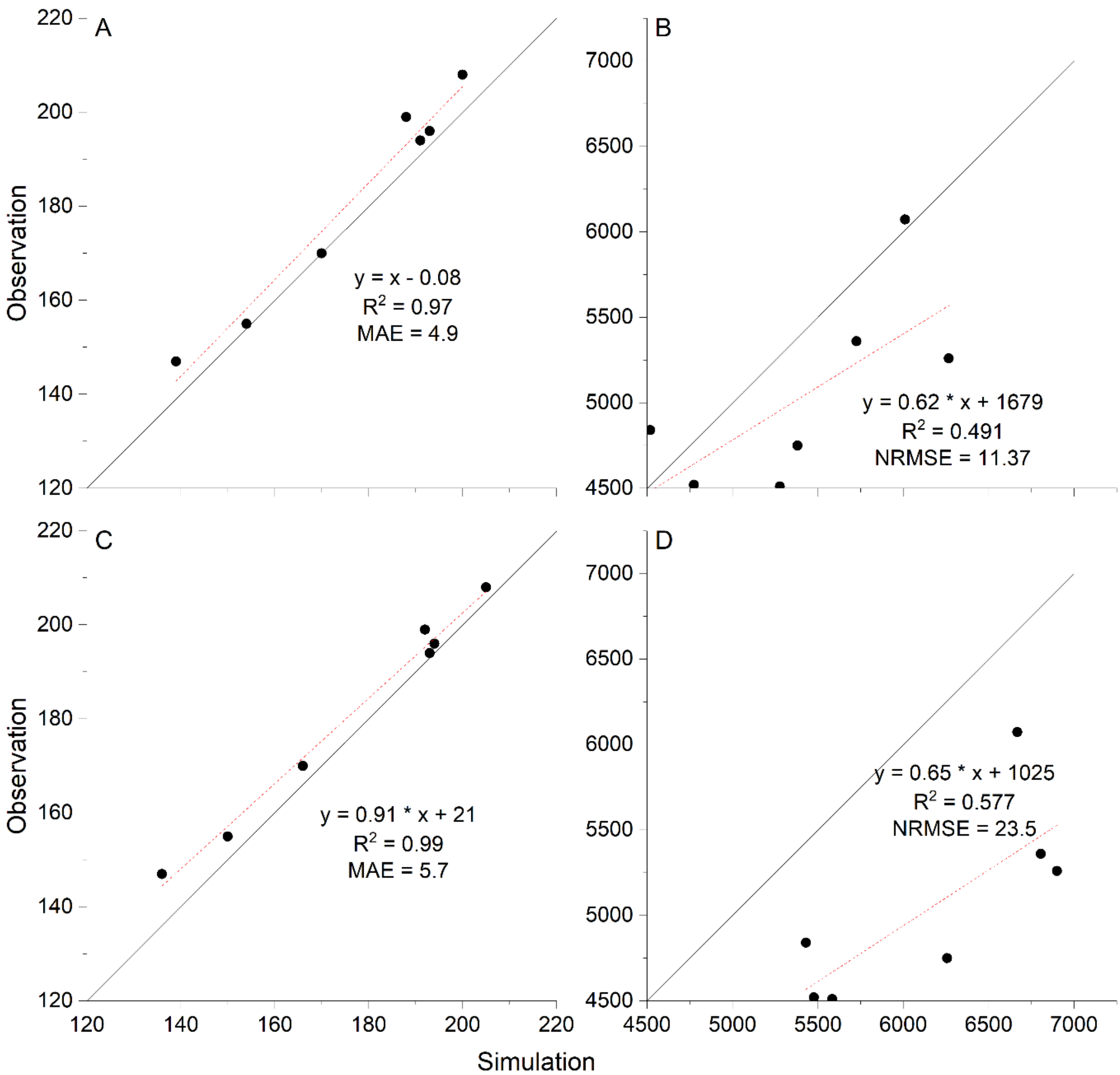

Fig. S6. Wheat simulation results for the validation dataset, showing (A, C) heading dates (days after planting) and (B, D) yield (kg ha^{-1}), using the default parameter sets. (A, B) *Yitpi* and (C, D) *Bacanora 88* represent the best and worst cases, respectively, among the default parameter sets.

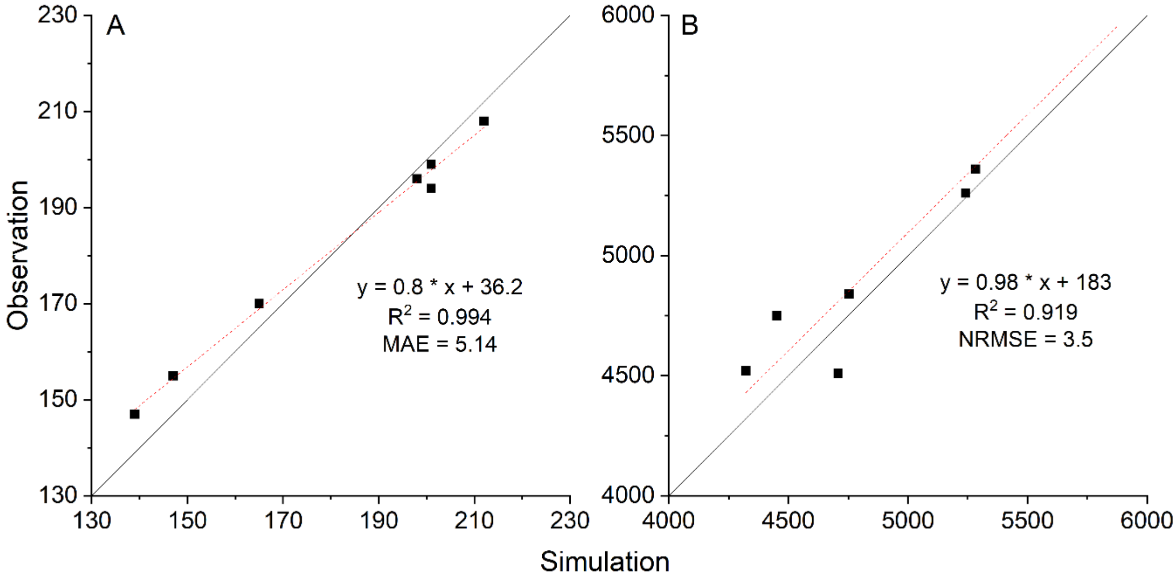

Fig. S7. Validation results for (A) heading dates (days after planting) and (B) yield (kg ha^{-1}), using the parameter values derived from the LOGO algorithm with five site combinations.

Reference

Beck, H.E., McVicar, T.R., Vergopolan, N., Berg, A., Lutsko, N.J., Dufour, A., Zeng, Z., Jiang, X., van Dijk, A.I., Miralles, D.G., 2023. High-resolution (1 km) Köppen-Geiger maps for 1901–2099 based on constrained CMIP6 projections. Scientific data 10, 724.

Dauphin, Y. N., Pascanu, R., Gulcehre, C., Cho, K., Ganguli, S., Bengio, Y., 2014. Identifying and attacking the saddle point problem in high-dimensional non-convex optimization. Advances in neural information processing systems 27.

Hyun, S., Joh, Y.S., Kim, K.S., 2025. Comparative Analysis of Wheat Cultivar Parameter Estimation Using Local Optimization Under Different Initial Values. Korean Journal of Agricultural and Forest Meteorology 27(4), 383-395.

Makowski, D., Wallach, D., Tremblay, M., 2002. Using a Bayesian approach to parameter estimation; comparison of the GLUE and MCMC methods. Agronomie 22(2), 191-203.

Wallach, D., Kim, K.S., Hyun, S., Buis, S., Thorburn, P., Mielenz, H., Seidel, S.J., Alderman, P.D., Dumont, B., Fallah, M.H., Hoogenboom, G., Justes, E., Kersebaum, K.-C., Launay, M., Leolini, L., Mehmood, M.Z., Moriondo, M., Jing, Q., Qian, B., Susanne, S., Seserman, D.-M., Shelia, V., Weihermüller, L., Palosuo, T., 2025. Evaluating the AgMIP calibration protocol for crop models; case study and new diagnostic tests. European Journal of Agronomy 168, 127659.